

Comparison of Electrochemical Activity of Nanosized α -LiFeO₂ Cathode Materials for Li-ion Secondary Battery Using Different Current Collectors

Jia Wang, Yourong Wang^{*}, Wei Zhou, Xiaofang Qian, Min Wang and Siqing Cheng^{*}

Innovation Center for Nanomaterials in Energy and Medicine (ICNEM), School of Chemical and Environmental Engineering, Wuhan Polytechnic University, Hubei 430023, P. R. China

^{*}E-mail: icnem@hotmail.com

Received: 3 March 2014 / Accepted: 18 March 2014 / Published: 14 April 2014

Nanosized α -LiFeO₂ cathode material for the Li-ion secondary battery using microporous carbon paper or aluminum current collectors was investigated. The results show that nanosized α -LiFeO₂ electrode using microporous carbon paper current collector exhibits much higher discharge capacity than that using aluminum current collector although the cell reaction mechanism is not dependent on the current collector. Moreover, the discharge capacity for the nanosized α -LiFeO₂ electrode using microporous carbon paper current collector at different discharge rate is approximately close. This may be attributed to the unique structure and electrochemical stability of microporous carbon paper.

Keywords: Nanosized α -LiFeO₂ cathode material; Current collector; Electrochemical activity; Lithium-ion batteries;

1. INTRODUCTION

Safe, low-cost and long-lasting rechargeable batteries are in high demand to address environmental and energy needs for energy storage systems.[1, 2] Due to its low toxicity, abundant resources, thermal safety and low cost, the lithium iron oxide (LiFeO₂) cathode material is of great potential for rechargeable lithium battery[3–7] although none of its compounds with various crystalline structure have proven to be stable when used as cathode nor capable of supporting extended cycling[8–12]. Therefore much more attention has recently been paid to the improvement on low capacity retention during cycling tests of LiFeO₂ as alternate cathode material for lithium secondary battery.

It has been shown that all these improved LiFeO₂ cathode materials are ascribed to the smaller size, which facilitates the contact between active materials and electrolyte and shorten lithium path.[7,

8, 12–15] α -LiFeO₂ nanoparticles with ~50 nm in size prepared by solid state reaction at 250 °C delivered a discharge capacity of 150 mAh g⁻¹ at 0.25 C in the range of 4.5-1.5 V after 50 cycles.[16] α -LiFeO₂ nanoparticles with ~10 nm in size synthesized by a molten salt route at 120 °C exhibited an initial discharge capacity of 71 mA h g⁻¹ at 2.0 C.[17] In our previous work, α -LiFeO₂ nanoparticle with 10 nm exhibited around 55.2% capacity retention with the discharge capacity of 101.5 mA h g⁻¹ after 50 cycles at 2 C.[18]

In addition, current collector should be crucially important for considering the improvement of cost, weight and performance of batteries. [19–21] Generally it is clear that the current collectors must be electrochemically stable in contact with the cell components over the operating potential window of the electrode. However, in practice, the typical current collectors, aluminum foil and copper foil, lead to a gradual increase in internal resistance of the battery due to their continued corrosion, with corresponding loss of the apparent capacity, at a given rate.[22, 23] Meantime, current collectors also reduce the gravimetric and volumetric energy densities of the battery. Accordingly, the suitable choice of current collector plays a crucial role on improvement of the performance of batteries.

In this study, microporous carbon paper and aluminum foil were employed as current collectors for Li-ion rechargeable battery with nanosized α -LiFeO₂ as cathode material and compared their electrochemical performance.

2. EXPERIMENTAL SECTION

Nanosized lithium iron oxide (α -LiFeO₂) were synthesized from LiOH·H₂O (Changzhou Chenhua Chemicals, 95.0%), LiNO₃ (Tianjin Kemiou Chemical Reagent, 99.0 %) and Fe (NO₃)₃·9H₂O (Tianjin Baishi Chemicals, 98.5%) by a simple molten salt method at room temperature. Stoichiometric amounts of the starting materials were thoroughly ground in a mortar with a pestle for 40 min. The mixture was transferred into a beaker on a constant temperature magnetic stirrer and stirred for 3 h at room temperature after drop-adding a certain amount of H₂O₂. The solid product was washed repeatedly with distilled water, ethanol, and dried at 80°C for 12 h.

Powder X-ray diffraction (XRD-6000, Shimadzu, Japan) using Cu K α radiation ($\lambda = 1.5418 \text{ \AA}$) at a scanning step of 2° per minute was used to identify the crystalline phase of the as-prepared lithium iron oxides. The particle size and morphology of the compound was observed with a field emission scanning electron microscopy (FE-SEM, Hitachi, Japan) and high resolution transmission electron microscope (HR-TEM, JEOL-2010, Japan) with an accelerating voltage of 200 kV.

The positive electrodes were fabricated by pasting the slurries of the as-prepared lithium iron oxide powder (70 wt%), acetylene black (20 wt%), and polyvinylidene difluoride (PVDF, 10 wt%) dissolved in N-methylpyrrolidone (NMP) on Al foil or microporous carbon paper strips by the doctor blade technique. Then the strips were dried at 80°C for 24 h in an air oven to remove water molecules. The electrolyte was 1 M LiPF₆ in a mixture of ethylene carbonate (EC)/diethyl carbonate (DEC) (1:1 by volume), the separator was CelgardR 2325. 2016 coin-type cells were assembled in an Ar-filled glove box using lithium metal foil as the counter electrode. The measurements of electrochemical performance were carried out on a program-controlled Battery Test System (Land®, Wuhan, China) at

room temperature. The cyclic voltammetry (CV) was conducted in a three-electrode cell with lithium foil as counter and reference electrodes by using a CHI660B Electrochemical Work-station (Chenghua, Shanghai, China) at room temperature.

3. RESULTS AND DISCUSSION

In this work, we used traditional molten salt method at room temperature to synthesize the nanosized α -LiFeO₂. [16, 24] Fig. 1 shows the powder X-ray diffraction pattern of the as-prepared sample. All diffraction peaks can be easily indexed to the pure cubic phase of α -LiFeO₂ (JCPDS 74-2284). Compared to standard diffraction peaks, the broadening reflections of the XRD indicate the small size of the products.

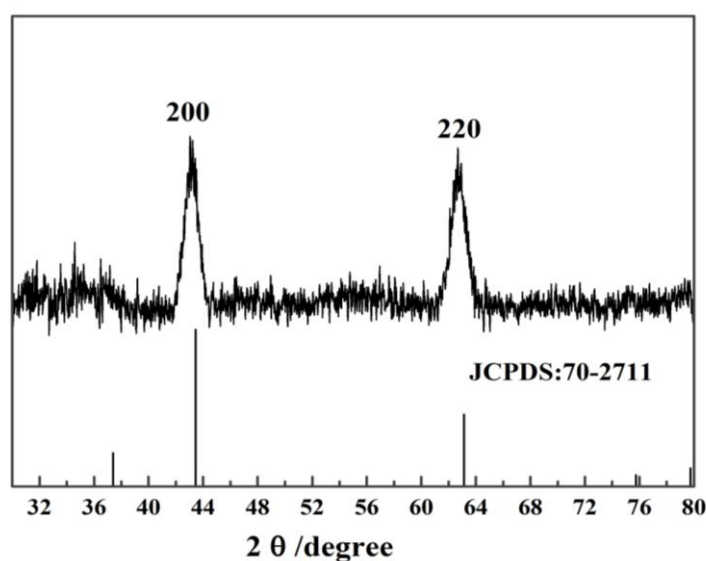


Figure 1. The X-ray diffraction pattern of the as-prepared sample

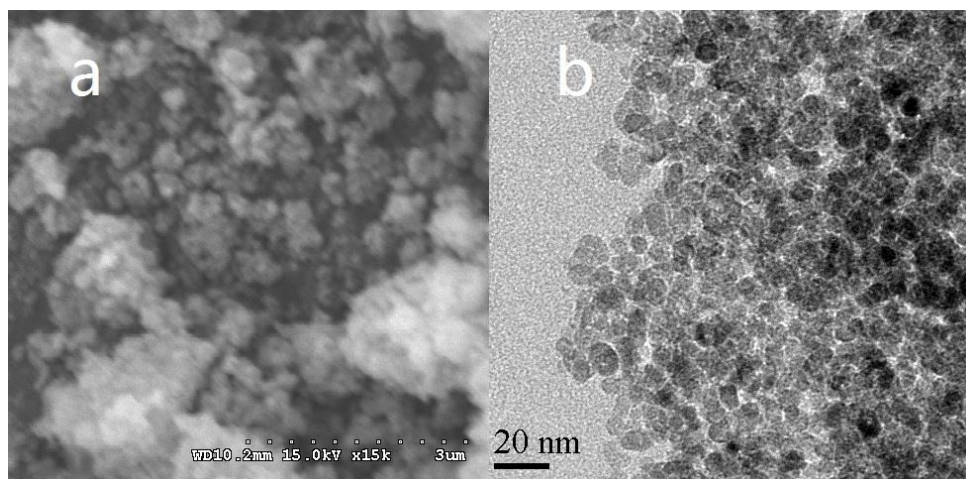


Figure 2. The SEM image of the α -LiFeO₂ powders

Based on the Debye–Scherrer equation[25], α -LiFeO₂ crystallite sizes could be calculated approximately at the marked peak (2 0 0) to be ca. 10.0 nm. The SEM image (Fig. 2a) shows that α -LiFeO₂ powder consists of large agglomerated nanoparticles with shortage of isolated particles adopting irregular morphology in this particular way. TEM investigation further reveals that α -LiFeO₂ powder consists of tiny particles of less than 10 nm in diameter with a spheroidal shape (Fig. 2b) and the particle size distribution is fairly narrow.

Fig. 3 shows the initial discharge curves of nanosized α -LiFeO₂ electrode using microporous carbon paper or aluminum current collector at different discharge current of 0.1, 1, 2 C. The initial discharge capacity of nanosized α -LiFeO₂ electrode using microporous carbon paper current collector (Fig. 3a) is 273.7, 269.6 and 276.3 mAh g⁻¹ at 0.1, 1 and 2 C, respectively, while the initial discharge capacity of sized α -LiFeO₂ electrode using aluminum current collector (Fig. 3b) is 197.6, 129.2 and

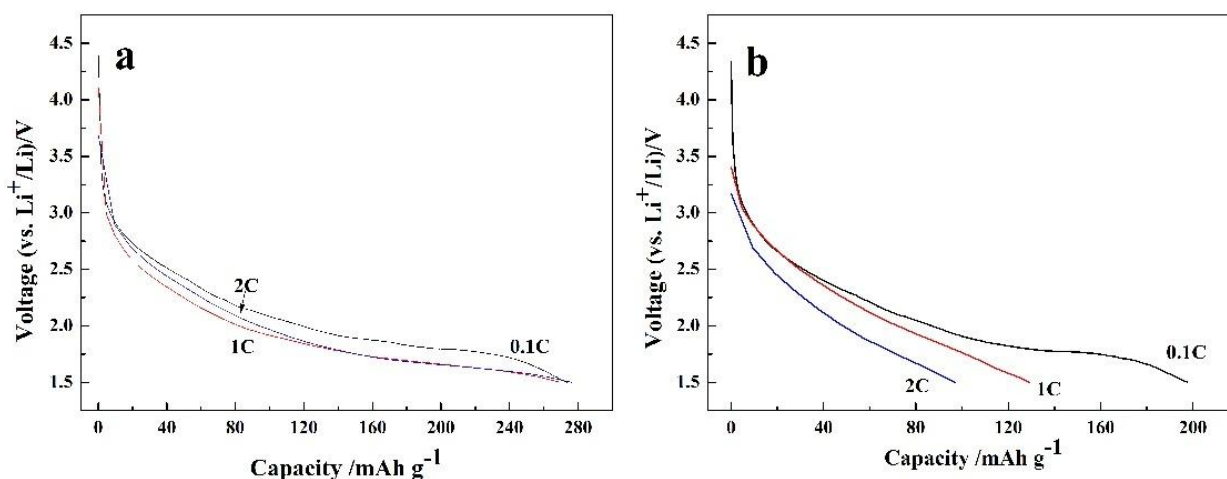


Figure 3. The initial discharge curves of nanosized α -LiFeO₂ electrode (a: microporous carbon paper ; b: aluminum current collector)

97 mAh g⁻¹ at 0.1, 1 and 2 C, respectively. As such, the discharge capacity of nanosized α -LiFeO₂ using microporous carbon paper current collector is much higher than that using aluminum current collector. This may be due to the favorable electron conduction when using microporous carbon paper current collector.[22] As shown as Fig. 4 for the electrochemical impedance spectra after charge/discharge for 4 cycles, the charge transfer resistance (R_{ct}) using microporous carbon paper current collector is significantly smaller than that using aluminum current collector by comparing the diameters of the semicircles. It is worth noting that the discharge capacities of nanosized α -LiFeO₂ using microporous carbon paper current collector at different current rate are very approximate while those using aluminum current collector are big different, indicating the high discharge capacity even at high current rate. This may due to easy creasing and tearing of aluminum current collector at high current rate[26] while the microporous carbon paper is electrochemically stable.

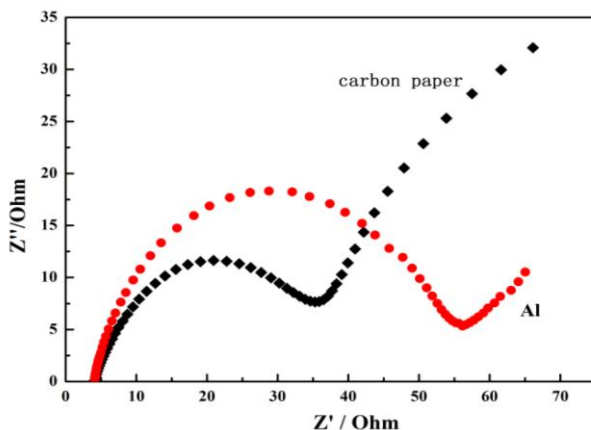


Figure 4. The electrochemical impedance spectra of nanosized α -LiFeO₂ on the different current collector

However, the charge-discharge curves of nanosized α -LiFeO₂ electrode using different current collectors exhibit approximate profile (Fig. 5a and Fig. 5b). As reported in previous work for the charge-discharge behavior of nanosized α -LiFeO₂ electrode, it has been persuaded strongly that orthorhombic LiFeO₂ underwent a structural change to spinel phase LiFe₅O₈ during the charge/discharge process, which resulted in the capacity fading of the Li/LiFeO₂ system, as similar in the orthorhombic Li/LiMnO₂ system for the capacity loss mechanism of the Li/LiMnO₂ cell due to the conversion from the orthorhombic to spinel structure. For the first four cycles of discharge curves of nanosized α -LiFeO₂ electrode using different current collector, cell voltage rapidly decreases to 3.4 V and then decreases slowly to the cut-off voltage of 1.5 V, a voltage plateau is displayed in 1.8-2.0 V.

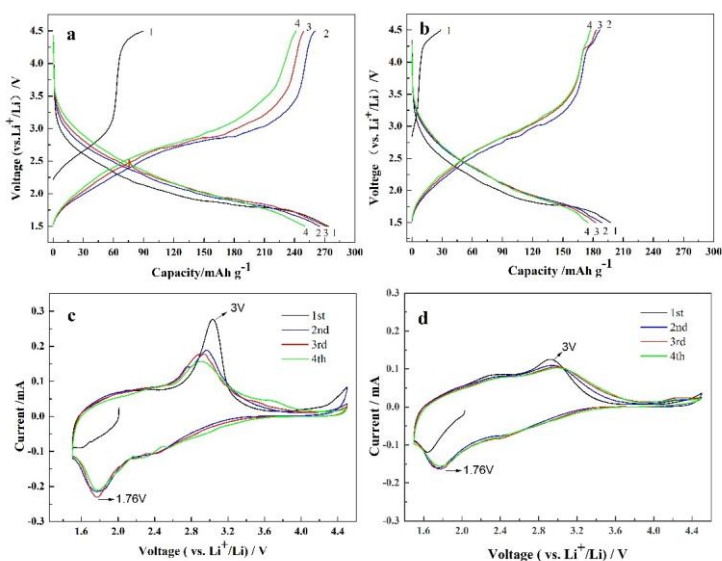


Figure 5. The charge-discharge curves and cyclic voltammograms of nanosized α -LiFeO₂ electrode on different current. a,c carbon paper ; b,d Al current collector

As such, current collector in electrode has no appreciable effect on the electrochemical reaction mechanism of electroactive materials. This could be further confirmed by cyclic voltammetry analysis for the first four cycles (Fig. 5c and Fig. 5d). The anodic peak at 3.0 V corresponds to the charge process while the cathodic peak at 1.75 V shows the subsequent discharge process. The unique difference in the charge-discharge curves of nanosized α -LiFeO₂ electrode using different current collectors lies in the discharge efficiency, resulting in the different discharge capacity. This also is identified in Fig.5 for the remarkable change in anodic peak at 3.0 V. The microporous carbon paper current collector facilitates the electron conduction in electrode, resulting in the higher discharge capacity.

Fig. 6 shows the capacity retention of the nanosized α -LiFeO₂ electrode using microporous carbon paper current collector at different discharge current of 1, 2C. The discharge capacity at different current rate decreases continuously upon cycling and the decreasing tendency becomes gradually slow to attain the cycling stability. It is 144.1 and 140.6 mAh g⁻¹ at 1 and 2 C, respectively, for the 100nd cycle, which is around 55.04% and 49.70% of the initial discharge capacity. More importantly, the discharge capacity tends to be close at different current rate. As mentioned above, this may result from the electrochemical stability of microporous carbon paper, exhibiting the potential in developing the nanosized α -LiFeO₂-based battery with the high discharge capacity at high current rate.

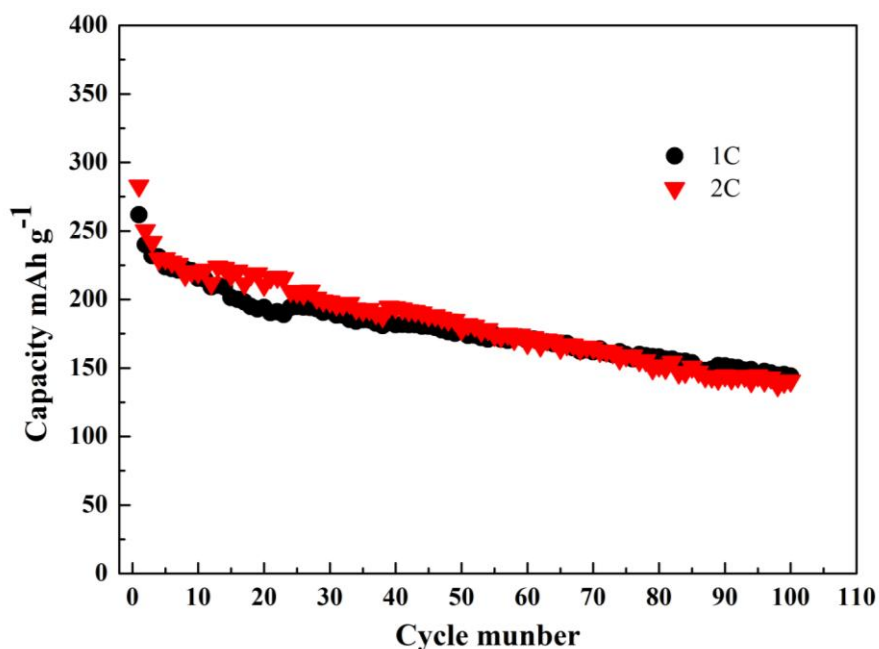


Figure 6. The cyclic stability of nanosized α -LiFeO₂ electrode

4. CONCLUSION

Electrochemical activity of nanosized α -LiFeO₂ cathode material for the Li-ion secondary battery using microporous carbon paper or aluminum current collectors was compared systematically.

It was found that the electrochemical activity is dependent on current collector. The nanosized α -LiFeO₂ cathode material for the Li-ion secondary battery using microporous carbon paper current collector exhibits much higher discharge capacity than that using common aluminum current collector, but current collector does not change electrochemical reaction mechanism. This is mainly due to the unique structure and electrochemical stability of microporous carbon paper compared to the common aluminum. More interestingly, the discharge capacity using microporous carbon paper is approximately close at different discharge rate, showing the favorable charge-discharge behavior using microporous carbon paper at high rate. Therefore, microporous carbon paper current collector exhibits the potential in developing the nanosized α -LiFeO₂-based battery with the high discharge capacity at high current rate.

ACKNOWLEDGEMENTS

This work is supported by Education Science Foundation of Hubei Province (No. Q20091806), Project of Chinese Ministry of Education (No. 208088).

References

1. P. Novák, K. Müller, K.S.V. Santhanam and O. Haas, *Chem. Rev.*, 97 (1997) 207.
2. L. Wang, X. He, J. Li, W. Sun, J. Gao, J. Guo and C. Jiang, *Angew. Chem. Int. Ed.*, 51 (2012) 9034.
3. V. Etacheri, R. Marom, R. Elazari, G. Salitra and D. Aurbach, *Energy Environ. Sci.*, 4 (2011) 3243.
4. M. Armand and J.-M. Tarascon, *Nature*, 451 (2008) 652.
5. M.S. Whittingham, *Chem. Rev.*, 104 (2004) 4271.
6. A.S. Aricò, P. Bruce, B. Scrosati, J.-M. Tarascon and W. van Schalkwijk, *Nat. Mater.*, 4 (2005) 366.
7. J.G. Li, J.J. Li, J. Luo, L. Wang and X. He, *Int. J. Electrochem. Sci.*, 6 (2011) 1550.
8. Y. Sakurai, H. Arai, S. Okada and J. Yamaki, *J. Power Sources*, 68 (1997) 711.
9. J.C. Anderson and M. Schieber, *J. Phys. Chem. Solids*, 25 (1964) 961.
10. Y. Sakurai, H. Arai and J. Yamaki, *Solid State Ion.*, 113–115 (1998) 29.
11. R. Kanno, T. Shirane, Y. Inaba and Y. Kawamoto, *J. Power Sources*, 68 (1997) 145.
12. J. Kim and A. Manthiram, *J. Electrochem. Soc.*, 146 (1999) 4371.
13. J. Morales, J. Santos-Peña, R. Trócoli, S. Franger and E. Rodríguez-Castellón, *Electrochimica Acta*, 53 (2008) 6366.
14. L. Bordet-Le Guenne, P. Deniard, A. Lecerf, P. Biensan, C. Siret, L. Fournès and R. Brec, *J. Mater. Chem.*, 9 (1999) 1127.
15. J. Wang, Y. Zhou, Y. Hu, R. O'Hayre and Z. Shao, *J. Mater. Sci.*, 48 (2013) 2733.
16. J. Morales and J. Santos-Peña, *Electrochem. Commun.*, 9 (2007) 2116.
17. Y. Ma, Y. Zhu, Y. Yu, T. Mei, Z. Xing, X. Zhang and Y. Qian, *Int J Electrochem Sci*, 7 (2012) 4657.
18. Y. Wang, J. Wang, H. Liao, X. Qian, M. Wang, G. Song and S. Cheng, *RSC Adv.*, 4 (2013) 3753.
19. A.H. Whitehead and M. Schreiber, *J. Electrochem. Soc.*, 152 (2005) A2105.
20. Y. Wang, H. Liao, J. Wang, Y. Zhu and S. Cheng, *Int. J. Electrochem. Sci.*, 8 (2013) 4002.
21. C. Iwakura, Y. Fukumoto, H. Inoue, S. Ohashi, S. Kobayashi, H. Tada and M. Abe, *J. Power Sources*, 68 (1997) 301.
22. Y.-S. Su and A. Manthiram, *Nat. Commun.*, 3 (2012) 1166.

23. L. Wang, X. He, J. Li, J. Gao, M. Fang, G. Tian, J. Wang and S. Fan, *J. Power Sources*, 239 (2013) 623.
24. X. Wang, L. Gao, F. Zhou, Z. Zhang, M. Ji, C. Tang, T. Shen and H. Zheng, *J. Cryst. Growth*, 265 (2004) 220.
25. M. Anis-ur-Rehman, A.S. Saleemi and A. Abdullah, *J. Alloys Compd.*, 579 (2013) 450.
26. L. Gaines and R. Cuenca, *ANLESD-42*, (<http://www.transportation.anl.gov>).

© 2014 The Authors. Published by ESG (www.electrochemsci.org). This article is an open access article distributed under the terms and conditions of the Creative Commons Attribution license (<http://creativecommons.org/licenses/by/4.0/>).